INT. J. CONTROL, 1998, VOL. 71, NO. 5, 807–821

Dynamics and control of entrained solutions in multi-mode Moore–Greitzer compressor models

J. SEAN HUMBERT†§ and ARTHUR J. KRENER‡

In this paper we investigate the behaviour of higher order Galerkin expansions of the Moore–Greitzer model of general transients in aeroengine compression systems. We assume steady state entrainment of the higher Fourier modes of the rotating stall cell which helps establish a framework for a simplified numerical analysis of the bifurcating solutions corresponding to rotating stall. For small values of the Greitzer surge parameter (B) we discuss general trends in the character of the pure stall solutions. The rotating stall characteristic is shown to exhibit deep hysteresis with a cubic compressor characteristic, establishing the fact that deep hysteresis to a certain extent is a multi-mode phenomena. Elimination of the hysteresis associated with the bifurcation into stall is accomplished in simulations with a combined feedback on the displacement from the peak of the compressor characteristic and the magnitude of the first mode amplitude of the stall cell. Behaviour for larger values of the B parameter is also investigated and novel surge/stall relaxation oscillations corresponding to classic surge are discovered.

1. Introduction

Rotating stall and surge are fluid dynamic instabilities which limit performance of axial compression systems. Deep surge is a time dependent axisymmetric flow characterized by oscillations in both pressure rise and mean flow. Pure rotating stall, on the other hand, is a steady (in the rotating frame), non-axisymmetric flow whose frequency is typically an order of magnitude higher than that of surge. The case where these two instabilities coexist is termed classic surge. Recovery from these conditions is characterized by hysteresis, where the throttle must be significantly opened past the point of inception of the instability in order to recover steady axisymmetric flow. The Moore–Greitzer equations are an attempt to model the non-linear phenomena of rotating stall and surge in these systems using first principles. The derivation of the complete set of equations can be found in Moore and Greitzer (1986).

The desired operating points of this system are those that provide the largest pressure rise across the compressor. However, increased susceptibility to surge and stall precludes operation at these setpoints. Reduced order ODE models of stall and surge phenomena provide a framework to assess the performance of various feedback controllers designed to minimize the harmful effects of rotating stall and surge. In previous work, Moore and Greitzer (1986) developed a single spatial harmonic expansion of the resulting equations. The bifurcations in this model were studied in

† Department of Control and Dynamical Systems, Mail Stop 107-81, California Institute of Technology, Pasadena, CA 91125, USA.
‡ Department of Mathematics, University of California, Davis, CA 95616, USA.
§ Corresponding author. e-mail: jshumber@indra.caltech.edu

0020-7179/98 $12.00

depth by McCaughan (1989). In recent research activity (Krener 1996, Liaw and Abed 1996, Banaszuk and Krener 1997, Krstic *et al.* 1998), feedbacks were shown to eliminate the hysteresis associated with the bifurcation into stall of this low order model. It was also shown in Henderson and Sparks (1996) that various feedbacks which eliminate hysteresis in the single mode expansion fail to do so when an additional spatial harmonic is included in the model.

In this paper we investigate the dynamics of multi-mode Galerkin expansions of the Moore–Greitzer equations. It is well known that unfolding the global bifurcation behaviour of systems of dimension three or greater is a formidable task. Hence, our goal in investigating these higher order expansions was not to document every intricacy of the models but rather develop a multi-mode framework that could be used to characterize the role of higher modes in both the uncontrolled dynamics and in the control design. In § 2 we introduce phase entrainment states which establish a framework for simple numerical analysis of non-axisymmetric periodic solutions. In § 3 we present a detailed numerical analysis of the three mode model (*MG*8) and note the general trends observed when more Fourier modes are included in the dynamics. In addition a feedback controller is presented which eliminates the hysteresis associated with the bifurcation into stall in the models we have simulated.

1.1. *Complete Moore–Greitzer model*

The complete model, whose derivation can be found in Moore and Greitzer (1986), is as follows

$$l_c \frac{\mathrm{d}\Psi}{\mathrm{d}\xi} = \frac{1}{4B^2}(\Phi - \Phi_T) \tag{1}$$

$$\Psi(\xi) = \Psi_c(\Phi + (\tilde{\phi}'_\eta)_0) - l_c \frac{\mathrm{d}\Phi}{\mathrm{d}\xi} - m(\tilde{\phi}'_\xi)_0 - \frac{\mu}{2}(2\tilde{\phi}'_{\xi\eta} + \tilde{\phi}'_{\eta\theta})_0 \tag{2}$$

$$l_c \frac{\mathrm{d}\Phi}{\mathrm{d}\xi} = -\Psi(\xi) + \frac{1}{2\pi}\int_0^{2\pi} \Psi_c(\Phi + (\tilde{\phi}'_\eta)_0)\,\mathrm{d}\theta \tag{3}$$

The dependent variables of this system are the annulus averaged pressure rise coefficient $\Psi(\xi)$, the annulus averaged axial flow coefficient $\Phi(\xi)$, and the upstream disturbance potential $\tilde{\phi}'(\eta, \theta, \xi)$, whose axial and circumferential partials give the local flow disturbance in the axial and circumferential directions. Independent variables include the time in wheel radians ξ, the circumferential coordinate θ, and the axial coordinate η. Equation (1) is an ODE in ξ which results from a mass balance of the plenum, (2) is a PDE in ξ and θ from the momentum balance of the system evaluated at the compressor face ($\eta = 0$), and (3) is an ODE in ξ which results from averaging out the circumferential dependence in (2). Note the subscript 0 denotes evaluation at $\eta = 0$, and the subscripts ξ, θ, η denote partial differentiation.

The compressor characteristic $\Psi_c(\Phi)$ is the response of the compressor for steady axisymmetric flow. For our analysis we will use the general cubic from Moore and Greitzer (1986):

$$\Psi_c(\Phi) = \Psi_0 + h\left[1 + \frac{3}{2}\left(\frac{\Phi}{w} - 1\right) - \frac{1}{2}\left(\frac{\Phi}{w} - 1\right)^3\right] \tag{4}$$

The throttle characteristic $\Phi_T(\Psi)$ represents the pressure loss across the throttle, assumed parabolic in Φ:

$$\Phi_T = (K_T + u)\sqrt{\Psi} \tag{5}$$

The variable u represents a feedback control on the operating point of the system. Parameters of the model define compressor geometry and operation characteristics. In our analysis we will focus on two parameters, K_T and B. The throttle coefficient K_T adjusts the position of the throttle, hence the operating point of the system. B is the Greitzer stability parameter which determines whether a given compressor is more likely to enter surge or rotating stall. Additional parameters are defined in Moore and Greitzer (1986). We will refer to the collection of parameters as

$$p = [K_T\ \Psi_0\ h\ w\ m\ l_c\ \mu\ B]' \tag{6}$$

1.2. *Previous work*

In Moore and Greitzer (1986) a single harmonic Galerkin expansion of the complete model was introduced. The reduced system of ODEs in non-dimensional time ξ are

$$\frac{d\Psi}{d\xi} = \frac{1}{4B^2 l_c}(\Phi - \Phi_T) \tag{7}$$

$$\frac{dA}{d\xi} = \frac{A}{m+\mu}\left(\frac{d\Psi_c}{d\Phi} + \frac{A^2}{8}\frac{d^3\Psi_c}{d\Phi^3}\right) \tag{8}$$

$$\frac{d\Phi}{d\xi} = \frac{1}{l_c}\left(\Psi_c - \Psi + \frac{A^2}{4}\frac{d^2\Psi_c}{d\Phi^2}\right) \tag{9}$$

The dependent variables of this model are the annulus averaged pressure rise coefficient $\Psi(\xi)$, the annulus averaged axial flow coefficient $\Phi(\xi)$, and the amplitude of the first spatial harmonic of rotating stall $A(\xi)$. $A = 0$ defines an invariant plane with steady (axisymmetric) solutions

$$\Phi = \Phi_T \tag{10}$$

$$\Psi = \Psi_c \tag{11}$$

For these fixed points the pressure rise across the compressor equals the pressure loss across the throttle, hence the operating point of the system is defined by the intersection of (4) and (5), shown in figure 1. The stability of these solutions depends on both the throttle coefficient K_T and the Greitzer surge parameter B. For larger values of the throttle coefficient K_T these axisymmetric solutions are stable, denoted with a solid line on figure 2. For our analysis in later sections we will be interested in small to medium ranges of the B parameter. For these cases the system loses linear stability with respect to axisymmetric perturbations via a supercritical *Hopf* bifurcation well after the system is throttled through the peak of the compressor characteristic. The bifurcated limit cycle is a relaxation oscillation in the Ψ and Φ states whose slow manifolds are the arms of the compressor characteristic Ψ_c, as shown in figure 2 (bottom, left).

The deep surge relaxation oscillation is the dominant behaviour for the larger B parameters. For small B parameters, however, the non-axisymmetric (A non-zero) case becomes dominant. As in the axisymmetric case for large throttle settings the system has a stable axisymmetric equilibrium defined by the intersection of the

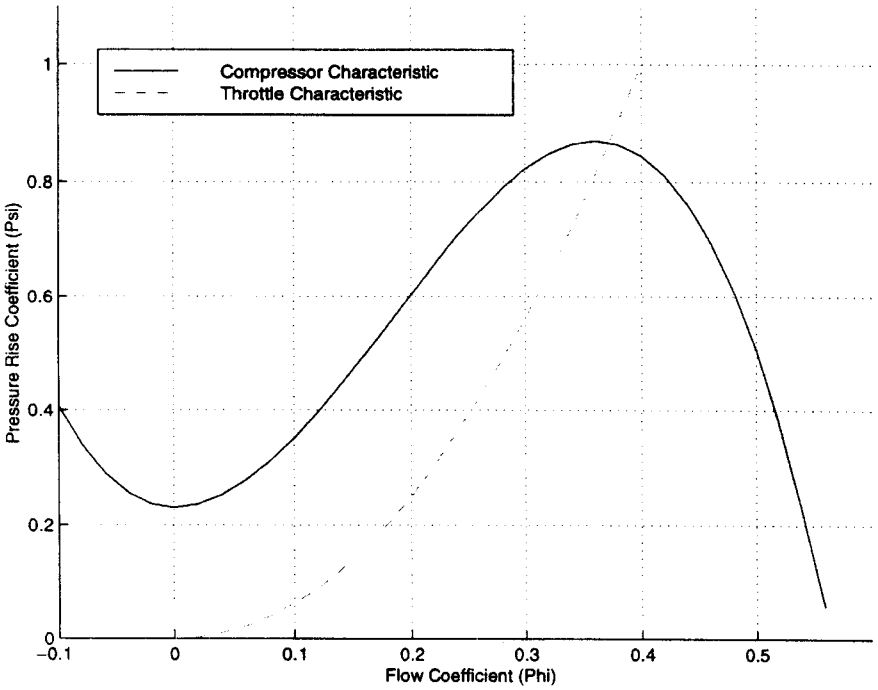

Figure 1. Compressor and throttle characteristics.

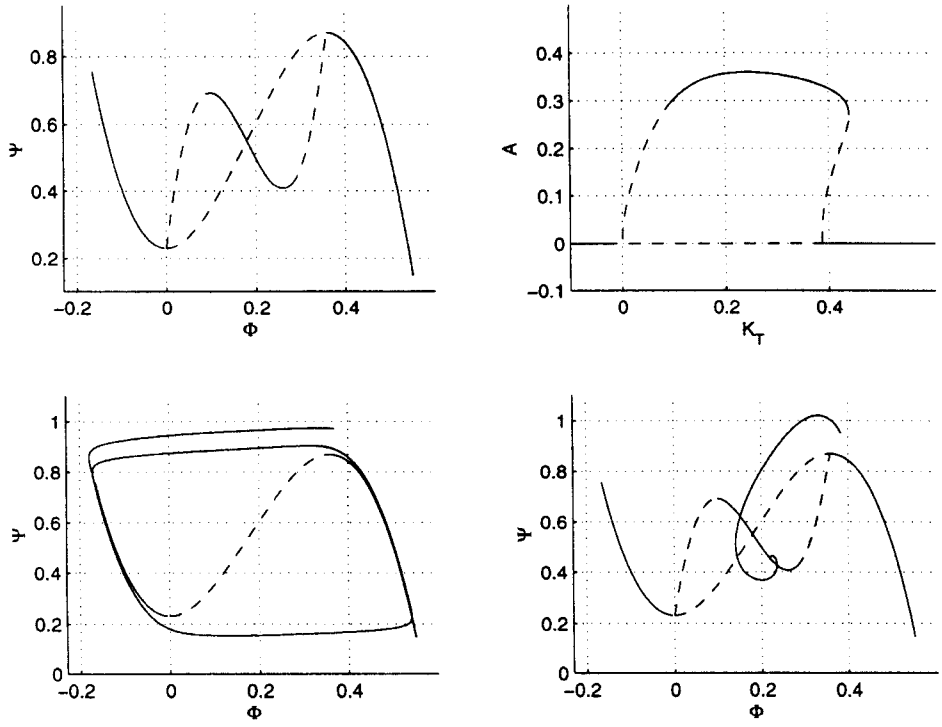

Figure 2. Dynamics of the single spatial harmonic approximation.

compressor and throttle characteristics. As the system is throttled through the peak of the compressor characteristic it loses linear stability with respect to non-axisymmetric perturbations via a *subcritical pitchfork* bifurcation. The new branch of equilibria is defined by

$$\Phi = \Phi_T \tag{12}$$

$$A = \left(-\frac{8\Psi_c'}{\Psi_c'''} \right)^{1/2} \tag{13}$$

$$\Psi = \Psi_c - \frac{2\Psi_c'\Psi_c''}{\Psi_c'''} \tag{14}$$

where the prime denotes differentiation with respect to Φ. In figure 2 we plot these equilibria on the (Φ, Ψ) and (A, K_T) planes. Stability is shown by linetype, solid (dashed) denoting stable (unstable) fixed points. Trajectories in this case approach steady non-axisymmetric solutions (rotating stall) as shown in figure 2 (bottom, right).

1.3. *Galerkin projections of the complete model*

In this section we discuss the application of the Galerkin method to reduce the infinite dimensional system (1–3) to a finite dimensional system of ODEs. Solutions to (2) are time dependent curves in the infinite dimensional space of functions of angle with periodic boundary conditions, $L_2[0, 2\pi]$. Our basic assumption is that the solutions of interest evolve in some finite dimensional subspace spanned by a truncated Fourier series approximation to the upstream disturbance potential:

$$\tilde{\phi}'(\xi, \theta, \eta) = \sum_{k=1}^{n} \frac{1}{k} \exp(k\eta)(A_k(\xi) \cos(k\theta - \Theta_k(\xi))) \tag{15}$$

Subtracting the circumferentially averaged dynamics (3) from (2) one has

$$0 = \tilde{\Psi}(\Phi, \xi, \theta) - m(\tilde{\phi}_\xi')_0 - \frac{\mu}{2}(2\tilde{\phi}_{\xi\eta}' + \tilde{\phi}_{\eta\theta}')_0 \tag{16}$$

where

$$\bar{\Psi} = \frac{1}{2\pi} \int_0^{2\pi} \Psi_c(\Phi + (\tilde{\phi}_\eta')_0)\, \mathrm{d}\theta \tag{17}$$

$$\tilde{\Psi} = \Psi_c(\Phi + (\tilde{\phi}_\eta')_0) - \bar{\Psi}(\Phi, \xi) \tag{18}$$

Following the procedure outlined in Krener (1996), we plug the truncated Fourier series for the upstream disturbance potential $\tilde{\phi}'$ into (16) to form a residual, and then integrate against $\cos(k\theta)$ or $\sin(k\theta)$. The resulting system has an independent variable of non-dimensional time ξ measured in rotor radians and dependent variables $A_k(\xi)$ and $\Theta_k(\xi)$, the amplitudes and phases of each spatial Fourier mode included in the truncation, respectively. The ODEs ($k = 1, \ldots, n$) are

$$\dot{A}_k = \frac{1}{\pi}\frac{k}{m+k\mu}\left[\int_0^{2\pi} \Psi_c(\Phi + (\tilde{\phi}'_\eta)_0)\cos(k\theta - \Theta_k)\mathrm{d}\theta\right] \tag{19}$$

$$\dot{\Theta}_k = \frac{k}{m+k\mu}\left[-\frac{\mu k}{2} + \frac{1}{\pi A_k}\int_0^{2\pi} \Psi_c(\Phi + (\tilde{\phi}'_\eta)_0)\sin(k\theta - \Theta_k)\mathrm{d}\theta\right] \tag{20}$$

2. General multi-mode remarks

These systems of dimension $2n+2$ are composed of two ODEs (1), (3) describing the time evolution of the annulus averaged flow coefficient Φ and the annulus averaged pressure rise coefficient Ψ, and $2n$ ODEs ($k = 1, \ldots, n$) for the time evolution of the amplitudes A_k and phases Θ_k of the n spatial Fourier modes of the stall cell:

$$\left.\begin{aligned}
\dot{\Psi} &= \frac{1}{4B^2 l_c}(\Phi - \Phi_T) \\
\dot{\Phi} &= \frac{1}{l_c}\left[-\Psi(\xi) + \frac{1}{2\pi}\int_0^{2\pi} \Psi_c(\Phi + (\tilde{\phi}'_\eta)_0)\,\mathrm{d}\theta\right] \\
\dot{A}_k &= \frac{1}{\pi}\frac{k}{m+k\mu}\left[\int_0^{2\pi} \Psi_c(\Phi + (\tilde{\phi}'_\eta)_0)\cos(k\theta - \Theta_k)\,\mathrm{d}\theta\right] \\
\dot{\Theta}_k &= \frac{k}{m+k\mu}\left[-\frac{\mu k}{2} + \frac{1}{\pi A_k}\int_0^{2\pi} \Psi_c(\Phi + (\tilde{\phi}'_\eta)_0)\sin(k\theta - \Theta_k)\,\mathrm{d}\theta\right]
\end{aligned}\right\} \tag{21}$$

The systems can be viewed as $n+1$ coupled oscillators $\dot{x} = f(x,p)$ with state and parameter vectors

$$x = [\Phi(\xi),\ \Psi(\xi),\ A_1(\xi),\ \Theta_1(\xi), \ldots, A_n(\xi),\ \Theta_n(\xi)]' \tag{22}$$

$$p = [K_T\ \Psi_0\ h\ w\ m\ l_c\ \mu\ B]' \tag{23}$$

We will begin our analysis by assuming a small B parameter and concentrating on the bifurcation behaviour defined by (21). As for the steady axisymmetric behaviour, it is similar to that of the single harmonic expansion. For large values of the throttle coefficient there is a stable axisymmetric equilibrium defined by the intersections of the compressor characteristic (4) and the throttle characteristic (5), as shown in figure 1. As the system is throttled down through the peak the axisymmetric equilibrium loses linear stability via a *multiple Hopf* bifurcation, as a pair of complex eigenvalues for each spatial mode of rotating stall simultaneously cross the imaginary axis with non-zero speed. Multiple periodic solutions bifurcate from this point, however there is only one branch that becomes stable for the range of throttle settings. Extensive simulations of (21) have shown that these stable periodic solutions decay to travelling waves where the phases of each mode increase linearly with time. This corresponds to the stall cell rotating around the annulus of the compressor with a fixed shape at steady state.

The remainder of this section will be dedicated to establishing a framework for analysis of bifurcated non-axisymmetric periodic solutions corresponding to rotating stall. First $SO(2)$ equivariance of multi-mode Moore–Greitzer models (21) will be established. With this property we will show that any phase combination appearing

in the dynamics must be harmonically balanced. This allows us to introduce phase difference states which reduces the problem of characterizing the non-axisymmetric equilibria to that of numerical continuation.

2.1. *SO(2) equivariance of multi-mode models*

In this section we will consider vector fields $\dot{x} = f(x)$ where f: $\mathbb{R}^{2n+2} \to \mathbb{R}^{2n+2}$. Let Γ be a symmetry group acting on $\mathbb{R}^{2n+2}$. The vector field $f(x)$ is *equivariant under the group* Γ if for every $\gamma \in \Gamma$ the following equation holds:

$$\frac{\partial \gamma}{\partial x}(x) f(x) = f(\gamma(x)) \tag{24}$$

Now consider Γ to be the continuous group of rotations $SO(2)$ on $\mathbb{R}^{2n+2}$. The *representation* of Γ on f: $\mathbb{R}^{2n+2} \to \mathbb{R}^{2n+2}$ is a simple rotation of the circumferential coordinate θ by a constant θ_0

$$\theta \longmapsto \theta + \theta_0 \tag{25}$$

The *action* of this group on polar coordinates is given by

$$(\Phi, \Psi, A_1, \ldots, A_n, \Theta_1, \ldots, \Theta_n) \longrightarrow (\Phi, \Psi, A_1, \ldots, A_n, \Theta_1 - \theta_0, \ldots, \Theta_n - n\theta_0) \tag{26}$$

We define new coordinates

$$(\Phi, \Psi, A_1, \ldots, A_n, \Theta_1, \zeta_1, \ldots, \zeta_{n-1}) \tag{27}$$

where

$$\zeta_i = \Theta_{i+1} - (i+1)\Theta_1$$

then the *action* of the group is given by

$$(\Phi, \Psi, A_1, \ldots, A_n, \Theta_1, , \zeta_1, \ldots, \zeta_{n-1}) \longrightarrow (\Phi, \Psi, A_1, \ldots, A_n, \Theta_1 - \theta_0, \zeta_1, \ldots, \zeta_{n-1}) \tag{28}$$

and the Jacobian of this transformation is everywhere the identity. Hence the equivariance condition (24) implies that the dynamics only depends on

$$\Phi, \Psi, A_1, \ldots, A_n, \zeta_1, \ldots, \zeta_{n-1}$$

and not Θ_1.

Definition 1: A general phase combination $\sum_{k=1}^{n} a_k \Theta_k$ appearing in the dynamics (21) is said to be *harmonically balanced* if $\sum_{k=1}^{n} a_k k = 0$.

We have shown the following:

Lemma 1: *Any phase combination appearing in the dynamics of multi-mode models* (21) *will be harmonically balanced.*

2.2. *Phase entrainment states*

As we mentioned previously, simulations show that stable non-axisymmetric solutions decay to travelling waves of fixed shape. We will refer to this phenomena as *entrainment*, or phase locking of the modes. In this situation, for a given mode, its amplitude is constant and the difference between its phase and the product of its harmonic number and the phase of the first mode would be constant:

$$\left.\begin{aligned} A_k &= \text{constant} \\ \zeta_k &= \Theta_{k+1} - (k+1)\Theta_1 = \text{constant} \end{aligned}\right\} \tag{29}$$

We find that during entrainment, Θ_1 is the only variable of the series which is a function of time. This is equivalent to the solutions (stall cells) rotating around the annulus with fixed shape.

In the above coordinates (27) we have seen that the dynamics does not depend on Θ_1. If we ignore Θ_1, we obtain a system with the following form:

$$\dot{z} = g(z, p) \tag{30}$$

$$z = [\Phi(\xi),\ \Psi(\xi),\ A_1(\xi), \ldots, A_n(\xi),\ \zeta_1(\xi), \ldots, \zeta_{n-1}(\xi)]' \tag{31}$$

$$p = [K_T\ \Psi_0\ h\ w\ m\ l_c\ \mu\ B]' \tag{32}$$

The fixed points of the system (30) are solutions of $g(z, p) = 0$. The polar coordinate representation of the dynamics is singular in the axisymmetric case ($A_k = 0, k = 1, \ldots, n$), hence we will focus on the character of the non-axisymmetric solutions for the range of throttle coefficients K_T. We will refer to these solutions as the entrained equilibria of the system:

$$g(z, K_T) = 0 \tag{33}$$

Intersections of the throttle characteristic (5) with these static equilibria (33) correspond to rotating stall limit cycles where the flow coefficient Φ, the pressure rise coefficient Ψ, the amplitudes of each spatial mode of the stall cell A_k, and the phase entrainment states ζ_i are all *constant*. Recall this corresponds to a stall cell (travelling wave) rotating around the annulus with fixed shape.

3. Entrained non-axisymmetric solutions

Typical parameters $[\Psi_0\ h\ w\ m\ l_c\ \mu] = [0.23\ 0.32\ 0.18\ 2.0\ 4.0\ 1.0]$ were chosen and the above systems (30) were analysed numerically in DSTool (see Back *et al.* 1992). In this section we present the results for the three mode model ($n = 3$) and also note the typical trends in the entrained dynamics as the order of the truncation of the disturbance potential is increased. Figure 3 (top, left) shows what we will refer to as the primary rotating stall equilibria traced out as the throttle coefficient K_T is varied. The compressor characteristic (4) is shown for reference. Intersections of the throttle characteristic (5) with the entrained stall equilibria correspond to travelling waves where the flow coefficient Φ, the pressure rise coefficient Ψ, the amplitudes of the first through third modes of rotating stall and their phase difference states are *constant*. Recall from § 1 this corresponds to the stall cell rotating around the annulus with fixed shape. Also shown in this figure are the bifurcation diagrams for the other five states including the amplitudes A_1, A_2 and A_3, and phase entrainments $\zeta_1 = \Theta_2 - 2\Theta_1$ and $\zeta_2 = \Theta_3 - 3\Theta_1$ as the throttle coefficient K_T is varied. Stability of these entrained solutions is denoted by either a solid line (stable) or a dashed line (unstable). Figure 4 is a plot of a stable solution ($K_T = 0.45$) versus angular position θ and nondimensional time ξ.

In addition to showing that the lower modes of rotating stall are predominant along this equilibria, from these diagrams we see evidence of a deep hysteresis associated with the primary bifurcation into stall. By deep hysteresis we simply mean that

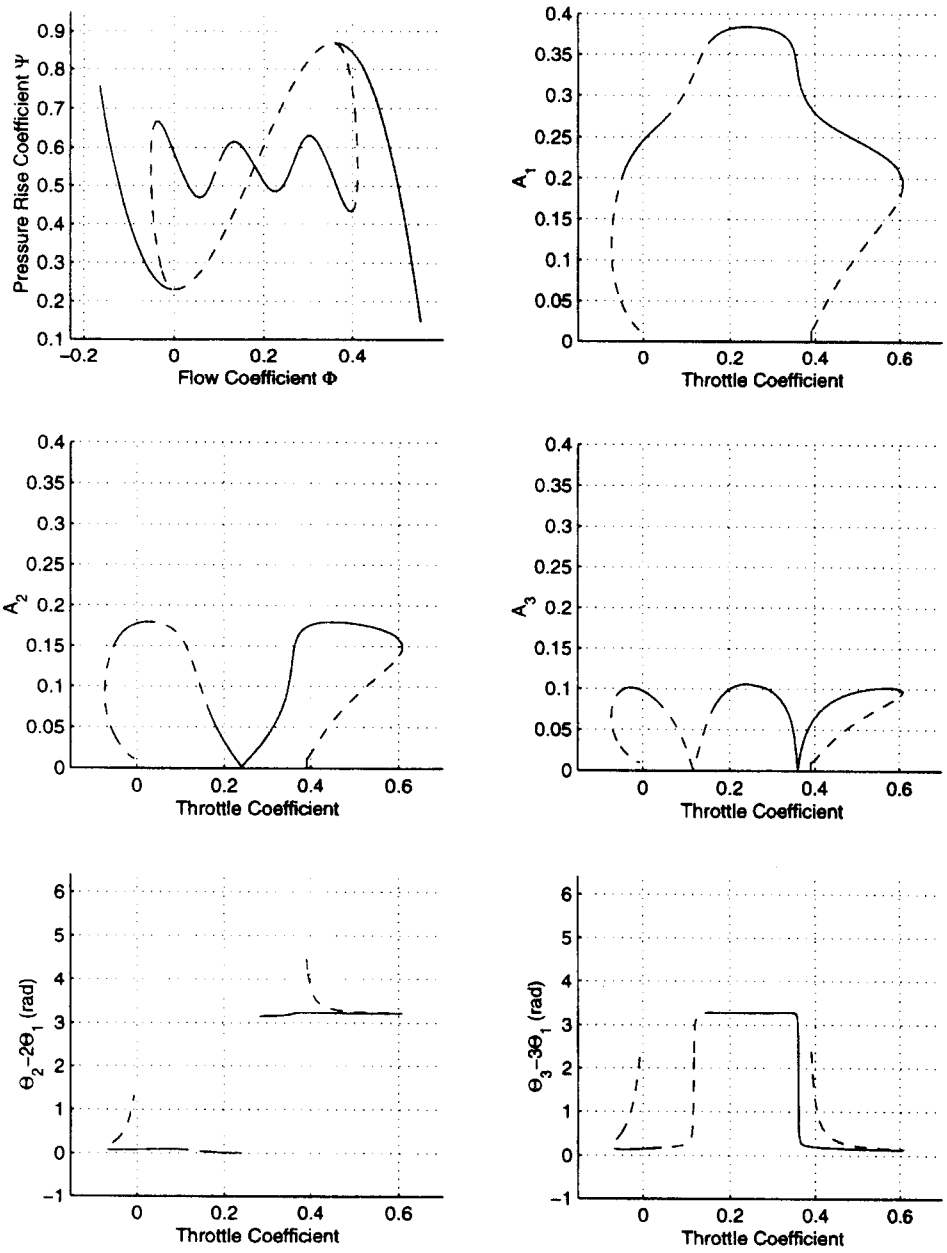

Figure 3. Primary stall equilibria—*MG*8.

stall equilibria exist for flow coefficients larger than that of the peak of the axisymmetric compressor characteristic. Previously in Banaszuk and Krener (1997) it was shown that in the single mode truncation (*MG*3) deep hysteresis depends on the *skewness* of the compressor characteristic. A characteristic is said to be left (right) skewed if it drops off faster to the right (left) of the peak. A right skewed characteristic is required for stall equilibria to exist to the right of the peak. With a continuous

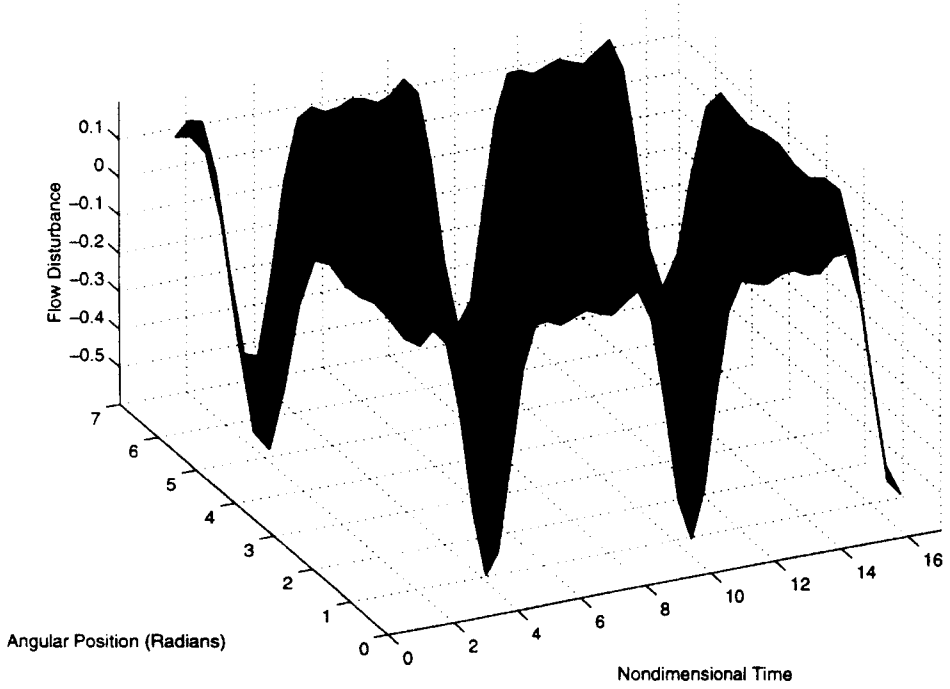

Figure 4. Stable rotating stall cycle—$MG8$.

cubic characteristic right skewness is not possible, hence higher degree characteristics were required for the one mode model to exhibit deep hysteresis. In this analysis we have assumed a cubic characteristic, hence these bifurcation diagrams show that deep hysteresis is to some extent a multi-mode phenomena.

In Wang *et al.* (1997) an attempt was made to include the deep hysteresis property in a low order ($MG3$) type model. Wang *et al.* introduced a non-polynomial modification to a cubic compressor characteristic, and the resulting stall characteristics exhibited deep hysteresis. However, there is no physical motivation for this approach to modelling deep hysteresis compressors. Our approach in this paper provides a physical explanation for the phenomena of deep hysteresis, i.e. higher modal stall cell content.

Upon comparison of the models we have simulated, including truncations of up to five Fourier modes, we see establishment of two trends in this primary rotating stall equilibria as we increase the order of the expansion. The extent of the deep hysteresis increases, as well as the number of relative minimums and maximums in the (Φ, Ψ) plane in the models we have investigated. These trends can be seen in figure 5 which shows plots of the primary stall characteristic for two, three, four and five mode models.

3.1. *Relaxation oscillations*

The Greitzer surge parameter B was also varied in DSTool, and both axisymmetric and non-axisymmetric relaxation oscillations were found. The typical

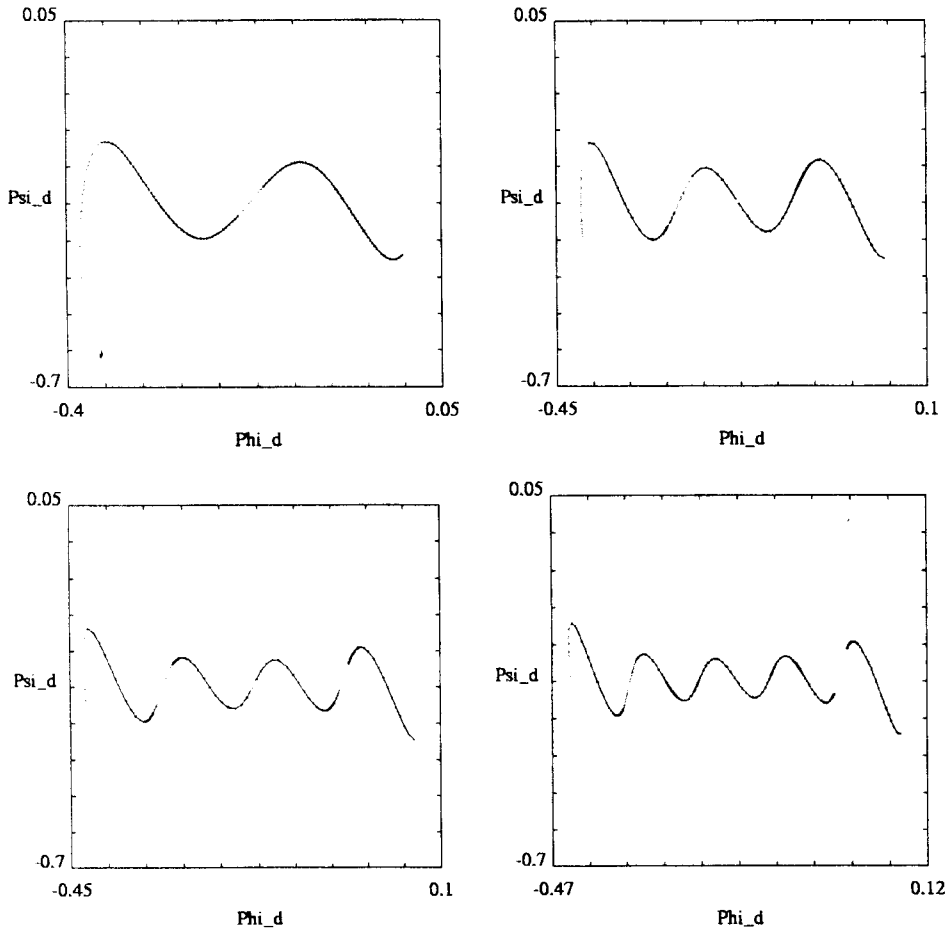

Figure 5. Primary rotating stall characteristic trends.

axisymmetric surge limit cycle exists for large (~ 1.0) B parameters, as shown in figure 6. Here $\Phi_d = \Phi - \Phi_e$, $\Psi_d = \Psi - \Psi_e$ and (Φ_e, Ψ_e) is the peak of the compressor characteristic. However, in the higher order Galerkin projections of the Moore–Greitzer model investigated in this paper, multiple inner relaxation oscillations were found to form around the relative minimums and maximums of the entrained rotating stall equilibria. Figure 6 shows trajectories that converge to these limit cycles for $K_T = 0.18$ and $K_T = 0.32$. The primary stall equilibria is shown for reference. In figure 7 we plot the flow coefficient Φ, the pressure rise coefficient Ψ, and the amplitudes of the first, second and third modes of rotating stall (A_1, A_2 and A_3) as functions of non-dimensional time ξ for the left trajectory that converges to the inner relaxation oscillation. From these time traces we see that this relaxation oscillation is actually *classic surge*, as stable oscillation occurs simultaneously in the surge and rotating stall states. We emphasize this inner relaxation oscillation is a novel phenomenon not found in the single mode expansion, and this phenomena exists for a much larger range of parameters than the classic surge type behaviour in McCaughan (1989).

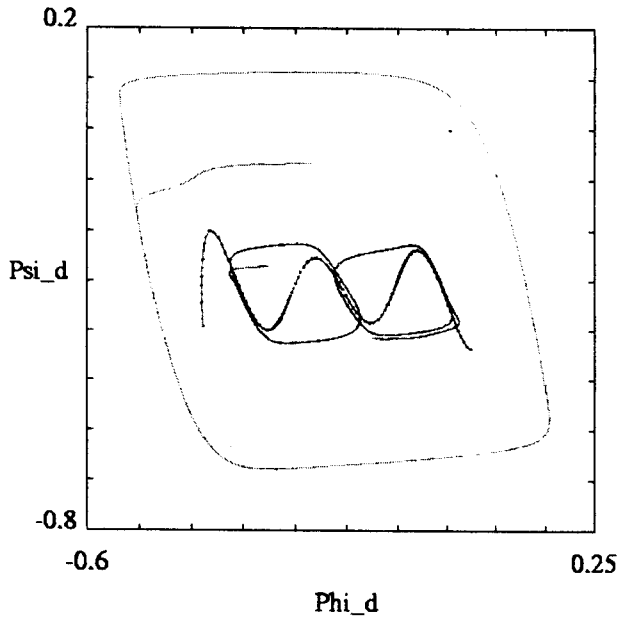

Figure 6. Relaxation oscillations—*MG*8.

3.2. *Elimination of hysteresis with feedback in multi-mode models*

It was shown previously in Krener (1995) that the feedbacks

$$u = K_\Phi(\Phi - \Phi_e) \tag{34}$$

$$u = K_\Psi(\Psi - \Psi_e) \tag{35}$$

each eliminate the hysteresis associated with the primary bifurcation into stall for the single harmonic expansion of the Moore–Greitzer model with a cubic compressor characteristic. Here K_Φ and K_Ψ denote gains and the subscript e denotes the desired operating point, i.e. the peak of the compressor characteristic. It was also shown in Banaszuk and Krener (1997) that with higher order right skew compressor characteristics feedback on the stall cell amplitude was required to eliminate hysteresis in the one mode expansion. The behaviour of these feedbacks (34, 35) in a two mode expansion was investigated in Henderson and Sparks (1996). Stabilization of the peak of the compressor characteristic was achieved, but the global property of hysteresis could not be eliminated.

Extensive simulations of the various control laws from previous papers mentioned were performed in the multi-mode framework developed in this paper. At this time we report that in the models we have simulated (up to five modes) feedback on a combination of the displacement from the peak of the compressor characteristic (34, 35) and the absolute value of the amplitude of the first mode eliminates the deep hysteresis associated with the primary bifurcation into stall:

$$u = K_\Phi(\Phi - \Phi_e) + K_\Psi(\Psi - \Psi_e) + K_{A_1}|A_1| \tag{36}$$

Figure 8 shows the results of implementing this feedback in the three mode expansion with gains of $K_\Phi = -2$, $K_\Psi = 2$ and $K_{A_1} = 9$. The top left figure is a

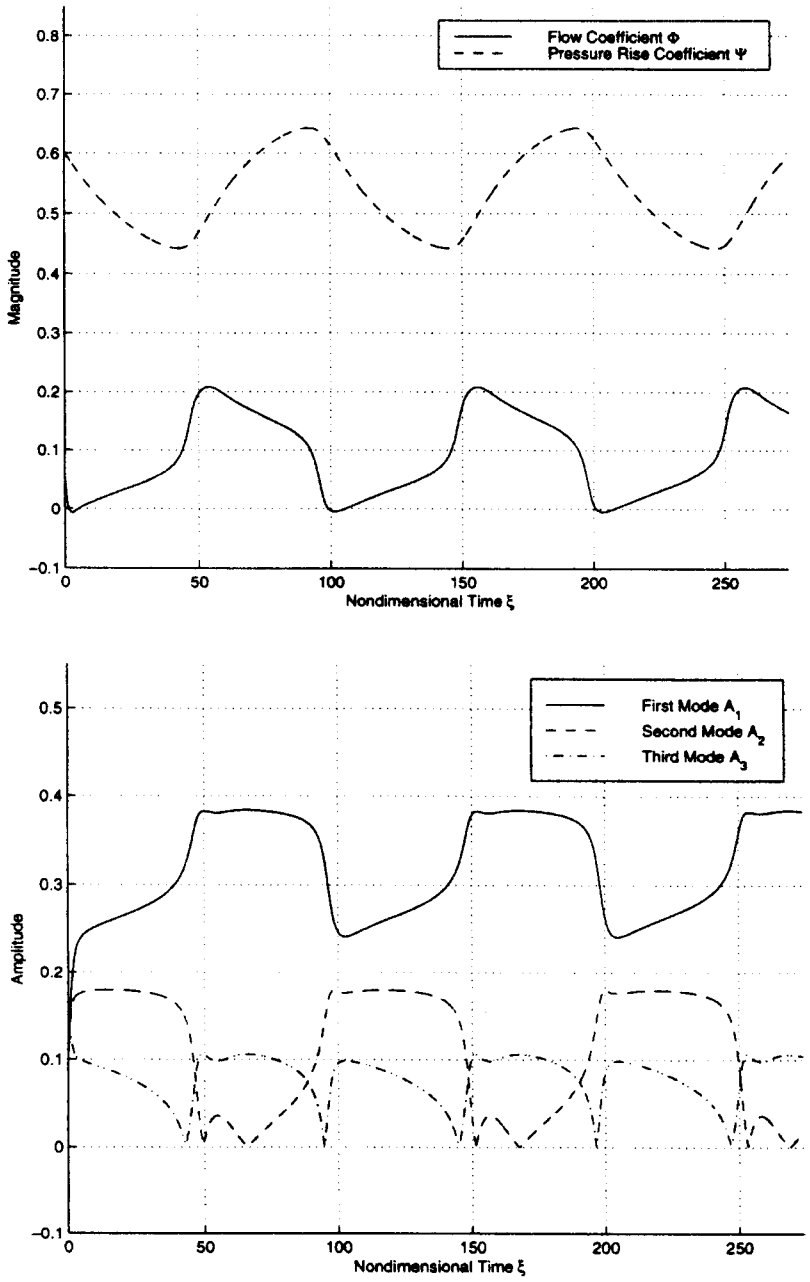

Figure 7. Classic surge relaxation oscillations—*MG*8.

plot of the stabilized rotating stall characteristic with the compressor characteristic (4) shown for reference. Also included are the bifurcation diagrams for the modal amplitudes (A_1, A_2 and A_3) and phase entrainment states (ζ_1, ζ_2) as the throttle parameter K_T is varied. We emphasize this was the simplest feedback that completely eliminated hysteresis. Feedback on higher modes was not required, but it

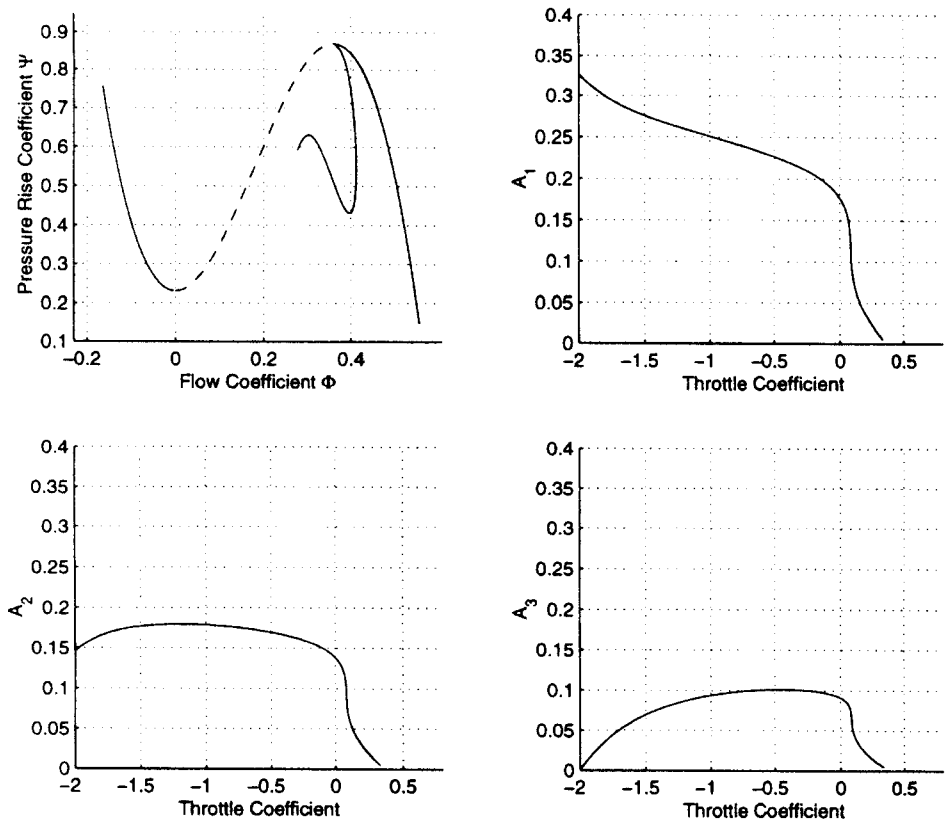

Figure 8. Controlled bifurcation diagrams—*MG*8.

did tend to decrease the equilibrium value of the stall amplitudes as the gains were increased.

4. Summary

We have discussed the dynamics of higher order Fourier expansions of the Moore–Greitzer model of transients in aeroengine compression systems. With the assumption of steady state entrainment a framework was established which simplified the numerical analysis of non-axisymmetric periodic solutions corresponding to rotating stall. The rotating stall characteristic was shown to exhibit deep hysteresis with a cubic compressor characteristic, establishing the fact that deep hysteresis to a certain extent is a multi-mode phenomena. General trends as the order of the models increased included an increase in the severity of the deep hysteresis and an increase in the number of relative minimums and maximums. New dynamic interactions (relaxation oscillations) of surge and stall representing classic surge were discovered in the higher order models. This framework also facilitated an evaluation of various bleed valve type feedbacks, and elimination of hysteresis associated with the bifurcation into stall was demonstrated in numerical simulations.

Acknowledgement

Support for this research was provided in part by AFOSR grant F49620-95-1-0409.

References

BACK, A., GUCKENHEIMER, J., MYERS, M., WICKLIN, F., and WORFOLK, 1992, *DSTool: Computer Assisted Exploration of Dynamical Systems*, AMS Notices, April.

BANASZUK, A., and KRENER, A., 1997, Design of controllers for MG3 compressor models with general characteristics using graph backstepping, *Proceedings of 1997 American Control Conference*, Albuquerque, pp. 977–981.

EVEKER, K., GYSLING, D., NETT, C., and SHARMA, O., 1995, Integrated control of rotating surge and stall in aeroengines. *SPIE Conference on Sensing, Actuation, and Control in Aeropropulsion.*

HENDERSON, E., and SPARKS, A., 1996, On the suitability of bifurcation stabilization control laws for high order Moore–Greitzer compressor models, preprint, September.

KRENER, A., 1995, *The Feedbacks which Soften the Primary Bifurcation of MG3*. Working Paper, September.

KRENER, A., 1996, *Revised Multi-Mode Moore–Greitzer Galerkin Compressor Models*. PRET Working Paper D96-8-15, August.

KRSTIC, M., FONTAINE, D., KOKOTOVIC, P., NETT, C., MYERS, M., GYSLING, D., and EVEKER, K., 1998, Useful nonlinearities and global stabilization of bifurcations in a model of jet engine surge and stall, *IEEE Transactions on Automatic Control*, to appear.

LIAW, D. C., and ABED, E. H., 1996, Active control of compressor stall inception: a bifurcation theoretic approach. *Automatica*, **32**, 109–115.

MCCAUGHAN, F. E., 1989, Bifurcation analysis of axial flow compressor stability. *SIAM Journal of Applied Mathematics*, **20**, 1232–1253.

MOORE, F. K., and GREITZER, E. M., 1986, A theory of post-stall transients in axial compression systems: part I—Development of equations. *Journal of Engineering for Gas Turbines and Power*, **108,** 68–76.

WANG, HSIN-HSUING, KRSTIC, M., and LARSEN, M., 1997, Control of Deep-hysteresis aeroengine compressors—part I: a Moore–Greitzer type model. *Proceedings of the American Control Conference, June.*